 CMES, vol.66, no.1, pp.73-99, 2010

Size-Dependent Behavior of Macromolecular solids II: Higher-Order Viscoelastic Theory and Experiments

D. C. C. Lam[1], L-H Keung[1] and P. Tong[2]

Abstract: Additional molecular rotations in long chained macromolecules lead to additional size dependence. In this investigation, we developed the higher order viscoelasticity framework and conducted experiments to determine the higher order material length scale parameters needed to describe the higher order viscoelastic behavior in the new framework. In the first part of the investigation of high order deformation behavior of macromolecular solids, the higher-order viscoelasticity theories for Maxwell and Kelvin-Voigt materials, and models of higher-order viscoelastic beam deflection creep are developed in this study. We conducted creep bending experiments with epoxy beams to show that the creep deflection behavior followed the conventional Kelvin-Voigt viscoelastic behavior when the beams are thick and that higher-order size dependences are present in both the time-independent elastic and time-dependent creep deflection when the beams are thin. The higher-order viscoelastic creep bending model with a higher-order material length scale parameter, l_2, was shown to be in good agreement with the data. Furthermore, l_2 is chain-based, instead of mechanism-based. Since each macromolecular solid has only a single set of chains, only a single l_2 is needed to characterize its higher order behavior in the newly developed higher order viscoelasticity framework. The new single l_2 higher order viscoelastic theory can be used to describe viscoelastic nanomechanical behaviors in nanostructured macromolecular solids.

Keywords: polymer, creep, viscoelastic, size effect, strain gradient

1 Introduction

Conventional descriptions of material behaviors are strain-based (Doi 1996). Chain rotation is the molecular mechanism underpinning strain-based deformation in macro-

[1] Department of Mechanical Engineering, the Hong Kong University of Science and Technology, Clear Water Bay, Hong Kong, People's Republic of China, Tel: (852)2358-8661, Fax: (852)2358-1543, Email: david.lam@ust.hk
[2] Bioengineering Department, University of California at San Diego, La Jolla, CA 92093-0412

molecular solid. Experiments have shown size-effects are present when strain gradients are non-negligible. Experiments showed that nanofibers 260 nm in diameter have an elastic modulus of 47 GPa while nanofibers 375 nm in diameter have an elastic modulus of 15 GPa in bending (Gu et al., 2005). Similar increases in the bending elastic modulus were reported by Cuenot et al. (2000) and Ji et al. (2006). Lam et al. (2003) and McFarland et al. (2005) experimentally found that the effective elastic modulus increased with the inverse square of the beam thickness. The increase in the elastic modulus was obtained when the data were analyzed using the conventional strain-based beam bending model. When the higher-order strain-gradient beam bending model with the higher-order bending parameter, b_h, was used, the elastic modulus was shown to remain constant. The high-order beam bending parameter, b_h,

$$b_h^2 = 3(1-\nu)l_2^2 + \frac{2(4-\nu)}{5}l_1^2 + 6(1-2\nu)l_0^2 \tag{1}$$

is dependent on Poisson's ratio, ν, the strain gradient material length scale parameters and l_0, l_1 and l_2, which are associated with dilatation gradients, stretch gradients and rotation gradients, respectively.

1.1 Molecular rotation and length-scale parameters

The size effects can be readily explained by higher order mechanics (Lam *et al.* (2003); Wang and Lam (2010)) with l_2 as the new material length scale parameter characterizing the size dependence. The higher order mechanics models have successfully explained the size-effects observed in bending beams and in nanocomposites. Despite the success of the mathematical higher order mechanics model, the molecular origin of the size-effects is lacking. This gap is filled by the breakthrough study detailed in part I of this series (Wei and Lam; 2010). The molecular deformation of beams in bending and tension were examined for three different polymers over a range of molecular weights using molecular models. The study showed that when the beams were strained uniformly in tension, the elastic modulus remained constant across different beam thicknesses. The behavior in bending was different. Experimental results indicated that the effective elastic moduli of beams in bending were increased by the strain gradients along the thickness direction. Molecular simulations revealed that the deformation energy during bending originated from molecular rotations. The increase in the effective elastic moduli was associated with increase in molecular rotations of the chains when rotation gradients are non-negligible. This means that the size-observed effect is not underpinned by a new mechanism, but is a new association of molecular rotations with rotation gradients. The association was tested by examining if l_2, the higher order material length scale parameter characterizing the rotation gradient behavior, shared the same inverse dependence on the segmental molecular weight as elastic modulus has. Simulation results confirmed that l_2 exhibited the same molecular weight dependence.

1.2 Higher-order viscoelastic behavior

For the first time, the molecular origin of the size effect in macromolecular solids was confirmed and validated. By using molecular mechanics, we were able to generate a new mathematical, physical and molecular framework relating the elastic deformation mechanism, the higher order elastic deformation mechanism, conventional mechanics and the higher order gradients mechanics together. However, a key element in the macromolecular behavior of higher order mechanics is missing. Along with time-dependent elastic deformation, macromolecular solids also deform viscoelastically. If the higher order elastic deformation has the same molecular chain rotation mechanism as the conventional strain-based elastic deformation mechanism, the higher order viscous part may also share the same chain sliding mechanism as the conventional viscous part.

In this paper, we developed a higher order viscoelastic framework and higher order bending models for beams. Creep deflections of beams with different thickness were then examined using nanometer-precision instrumentations to show that the size-dependence is also present in the time-dependent creeping regime. The development of the framework, beam models, experimental designs and results are detailed in the section below.

2 Strain gradient viscoelasticity

In the first part of this paper, a brief summary of strain gradient visoelasticity theory is given. Beam bending solutions for a Maxwell material and a Kelvin-Voigt material for load relaxation after deflection, creeping deflection at constant load and oscillatory loading are developed using the theory.

Higher-order theories of plasticity and elasticity, which include contributions from strain gradients, have been developed by many authors. Lam *et al.* (2003) developed a linear elastic bending theory for plane-strain beams. In this part of the paper, the foundation of higher-order viscoelasticity is first summarized. Solutions for oscillations, relaxation and creep are developed for Maxwell and Kelvin-Voigt materials.

In the derivation of strain gradient theory for viscoelasticity, we shall use the same set of strain/stress decompositions and definitions used in strain gradient elasticity. In this theory, the strain tensor is ε_{ij}; and the second-order deformation gradient tensors are the dilatation gradient vector, γ_i, the deviatoric stretch gradient tensor,

η_{ijk}, and the symmetric rotational gradient (curvature) tensor, . There are six independent components in ε_{ij}, three in γ_i, seven in η_{ijk}, and five in χ_{ij}, which gives a total of 15 independent components in the second-order deformation gradient tensors. The stress measures, the work-conjugates to the strain measures, are the classical stress tensor, $\sigma_{ij,}$ and the higher-order stresses, p_i, τ_{ijk} and m_{ij}. A summary of the strain gradient elasticity theory and the constitutive relations for linear elastic center-symmetric isotropic materials is given in Appendix I.

For linear isotropic viscoelastic materials, the constitutive relations in differential equation forms (Fung and Tong, 2001) can be written as

$$P_3(\frac{\partial}{\partial t})\sigma_{kk} = 2Q_3(\frac{\partial}{\partial t})\varepsilon_{kk} \tag{2}$$

$$P_4(\frac{\partial}{\partial t})\sigma'_{ij} = 2Q_4(\frac{\partial}{\partial t})\varepsilon'_{ij} \tag{3}$$

$$P_0(\frac{\partial}{\partial t})p_i = 2l_0^2 Q_0(\frac{\partial}{\partial t})\varepsilon_{mm,i} \tag{4}$$

$$P_1(\frac{\partial}{\partial t})\tau_{ijk} = 2l_1^2 Q_1(\frac{\partial}{\partial t})\eta_{ijk} \tag{5}$$

$$P_2(\frac{\partial}{\partial t})m^s_{ij} = 2l_2^2 Q_2(\frac{\partial}{\partial t})\chi^s_{ij}, \tag{6}$$

where $\sigma'_{ij}, \varepsilon'_{ij}$ are the stress and strain deviations, and Ps and Qs are polynomials of the time-derivative operator.

For a spring and a dashpot in series (Maxwell model), the polynomials of the operator are

$$P_0 = P_1 = P_2 = 1 + \eta_g \frac{\partial}{\partial t} \tag{7}$$

$$P_3 = P_4 = 1 + \eta \frac{\partial}{\partial t} \tag{8}$$

$$Q_0 = Q_1 = Q_2 = \mu_g \left[1 + \eta_g \left(1 + \frac{\mu_{1g}}{\mu_g}\right) \frac{\partial}{\partial t}\right] \tag{9}$$

$$Q_3 = \frac{1+\nu}{3+(1-2\nu)} Q_4 = \frac{1+\nu}{3+(1-2\nu)} \mu \left[1 + \frac{\mu_1}{\mu} \frac{\partial}{\partial t}\right], \tag{10}$$

where η and η_g are the viscosity coefficients, μ and μ_g are the first shear moduli, and μ_1 and μ_{1g} are the second shear moduli associated with strains and strain gradients, respectively. The viscosity coefficients have the dimension of time.

3 Bending Theory for Plane-Strain Beams

3.1 Approach

In the development of a bending theory for plane strain beams (Lam *et al.,* 2003), the mid-plane of the thin plane-strain beam (an infinitely wide plate) is the *x*-*y* plane of a Cartesian coordinate system with the width direction along the y-axis. The beam thickness is much smaller than the length and width. The displacement along the width direction is ignored and the beam deformation is assumed to be independent of the width coordinate, *y*. Only the normal tractions are applied on the top or bottom surfaces of the beam and the body force is ignored. In the derivation, the bending stress resultants are first defined in terms of the stress measures. Then, the bending equilibrium equations and the prescribed force boundary conditions are derived. Afterwards, a new set of bending deformation measures is proposed to establish the bending constitutive relations using Taylor expansions of displacements with respect to the beam thickness.

3.2 Equilibrium Relations

In deriving the equilibrium relations and force-prescribed boundary conditions, we define the stress resultants with higher-order stress measures as

$$\begin{aligned}
N &= \int_{-h/2}^{h/2} \sigma_{11} dz; \\
Q &= \int_{-h/2}^{h/2} \left(\sigma_{13} + \frac{1}{2}\partial_1 m_{12} - \partial_1 \tau_{113} \right) dz; \\
M &= \int_{-h/2}^{h/2} (z\sigma_{11} + m_{12} + p_3 + \tau_{113}) dz; \\
N^h &= \int_{-h/2}^{h/2} (p_1 + \tau_{111}) dz; \\
M^h &= \int_{-h/2}^{h/2} z(p_1 + \tau_{111}) dz
\end{aligned} \tag{11}$$

where N is the axial stress resultant per unit width, Q is the shear stress resultant per unit width, and M is the moment per unit width in the beam. New higher-order stress resultants per unit width, N^h, and the higher-order moment resultant per unit width, M^h, are introduced to account for the higher-order effect. The resultant shear stress, Q, and the moment, M, now contain higher-order stress terms.

We consider only the deformations along the length and thickness directions of the beam and assume that the beam deformation is independent of the coordinate, *y*.

Combining the equilibrium equations in Eq. (C1), we obtain the boundary conditions from Eq. (C2) and the stress resultant definitions Eq. (C3)

$$\frac{\partial N}{\partial x} - \frac{\partial^2 N^h}{\partial x^2} = \rho h \frac{\partial^2 u}{\partial t^2} \tag{12}$$

$$\frac{\partial Q}{\partial x} + \bar{q} = \rho h \frac{\partial^2 w}{\partial t^2}; \quad \frac{\partial M}{\partial x} - \frac{\partial^2 M^h}{\partial x^2} - Q = 0 \tag{13}$$

where $\bar{q} = \bar{q}_{h/2} + \bar{q}_{-h/2}$. Equation (13) can be re-written as

$$\frac{\partial^2 M}{\partial x^2} - \frac{\partial^3 M^h}{\partial x^3} + \bar{q} = \rho h \frac{\partial^2 w}{\partial x^2}. \tag{14}$$

In Eq. (12)-(14), we ignore the variation of u and w through the beam thickness in the inertia terms. The solution of Eqs. (12)-(13) satisfies the equilibrium equation (C1), and the top and bottom boundary conditions, Eq.(C2).

The stress resultants at the traction prescribed boundaries are derived from Eqs. (57) and (58) of Lam et al. (2003) as

$$N - \frac{dN^k}{dx} = \bar{N} = \int_{-h/2}^{h/2} \bar{t}_1 dz + \bar{P}_1|_{z=-h/2} + \bar{P}_1|_{z=h/2} \tag{15}$$

$$Q = \frac{\partial M}{\partial x} - \frac{\partial^2 M^h}{\partial x^2} = \overline{Q} = \int_{-h/2}^{h/2} \bar{t}_3 dz + \bar{P}_3|_{z=h/2} - \bar{P}_3|_{z=-h/2} \tag{16}$$

$$M - \frac{dM^h}{dx} = \bar{M} = \int_{-h/2}^{h/2} (z\bar{t}_1 + \bar{g}_2) dz - \frac{h}{2}\bar{P}_1|_{x=-h/2} + \frac{h}{2}\bar{P}_1|_{x=h/2} \tag{17}$$

$$N^h = \overline{N}^h = \int_{-h/2}^{h/2} \bar{r} dz; \quad M^h = \overline{M}^h = \int_{-h/2}^{h/2} \bar{r} z dz, \tag{18}$$

where $\bar{N}$ is the prescribed total axial force in units of N/m; $\bar{Q}$ is the prescribed shear force in units of N/m; $\bar{M}$ is the prescribed moment per unit width in units of N-m/m; $\bar{N}^h$ is the prescribed higher-order axial force in units of N-m/m; and $\bar{M}^h$ is the prescribed higher-order moment per unit width in units of N-m^2/m. The quantities $\bar{t}'$s, $\bar{g}'$s, $\bar{r}$ and $\bar{P}'$s are defined in Eqs. (57) and (58) of Lam *et al.* (2003). With pure bending, both $\bar{N}$ and $\bar{N}^h$, which correspond to pure tension, are both zero.

In brief, the independent stress resultant measures for bending are the moment, M, and the higher-order, moment, M^h. The shear force, Q, is associated with M and M^h (Eq.(13)). The equations detailed in this section are used in the following section for development of the bending equations.

3.3 Deformation and Constitutive Relations

The deformation measures and constitutive relations for thin beams can be established by expanding the displacements as a power series of the beam thickness, h,

$$u = \sum_{i=1}^{\infty} u_i(x,s,t)h^i; \quad v = 0; \quad w = \sum_{i=1}^{\infty} w_i(x,s,t)h^i, \tag{19}$$

Here $s = z/h$ and z is the coordinate in the thickness direction. The expansion of the non-vanishing strains and strain gradients are given in Eq. (A1) of Lam *et al.* (2003) with

$$\frac{\partial u_0\,(x,s,t)}{\partial s} = \frac{\partial w_0\,(x,s,t)}{\partial s} = \frac{\partial^2 u_1\,(x,s,t)}{\partial s^2} = \frac{\partial^2 w_1\,(x,s,t)}{\partial s^2} = 0 \tag{20}$$

to ensure that the strains and strain gradients are only of order 1 or smaller as $h \to 0$. Then, the non-vanishing stresses and higher-order stresses, and the expansion of the second boundary equation of Eq. (C2) and the first and second equilibrium equations of Eq. (C1) in terms of displacements are given in Appendix D.

Defining the curvature, κ, and the curvature gradient, κ_h, respectively, as

$$\kappa = -w_0''(x); \quad \kappa^h = -w_0'''(x), \tag{21}$$

we obtain, for bending of beams only, the constitutive equations for the non-vanishing stresses and higher-order stresses in terms of the curvature and the curvature gradients (Appendix D).

The constitutive relations for beam bending are obtained by substituting Eqs. (D15)–(D18) into Eq. (C2). This gives the constitutive relations as

$$M = -D_0 D_1 \kappa - D_0 D_2 \frac{\partial \kappa^h}{\partial x}, \quad M^h = -D_0 D_3 \kappa^h, \tag{22}$$

where D_0D_1, D_0D_2 and D_0D_3 are the bending rigidities with

$$D_0 = \frac{\mu h^3}{6(1-\nu)}; \quad D_1 = \frac{1}{\mu}\left[Q_c \frac{\partial}{\partial t} + \frac{b_h^2}{h^2} Q_g \frac{\partial}{\partial t}\right];$$

$$D_2 =$$

$$\frac{1}{\mu}\left\{-\frac{h^2}{20} Q_c \frac{\partial}{\partial t} + \left[\frac{1}{8} l_2^2 + \left(\frac{13}{60} - \frac{\nu}{15} + \frac{\nu^2}{20}\right)\frac{l_1^2}{1-\nu} + \frac{(1-2\nu)(3-\nu)}{4(1-nu)} l_0^2\right] Q_g \frac{\partial}{\partial t};\right.$$

$$D_3 = \frac{1}{2\mu}\left[\frac{4-\nu}{5}l_1^2 + (1-2\nu)l_0^2\right]Q_g\frac{\partial}{\partial t}; \tag{23}$$

$$b_h^2 = 3(1-\nu)l_2^2 + \frac{2(4-\nu)}{5}l_1^2 + 6(1-2\nu)l_0^2, \tag{24}$$

in which D_0 is the conventional bending rigidity and D_1, D_2, D_3 and b_h are the higher-order bending parameters, which characterize the thickness dependence of beam bending. The bending equation (14) can be written as

$$-D_0D_1\frac{\partial^4 w_0}{\partial x^4} + D_0(D_3 - D_2)\frac{\partial^6 w_0}{\partial x^6} + \bar{q} = \rho h\frac{\partial^2 w_0}{\partial t^2}. \tag{25}$$

From Eqs. (16)–(18), the boundary conditions become

$$Q = \frac{\partial M}{\partial x} - \frac{\partial^2 M^h}{\partial x^2} = \bar{Q} \text{ or } w_0 = \bar{w}_0, \tag{26}$$

$$M - \frac{\partial M^h}{\partial x} = barM \text{ or } \frac{\partial w_0}{\partial x} = \bar{w}_0' \tag{27}$$

$$M^h = 0 \text{ or } \frac{\partial^2 w_0}{\partial x^2} = \bar{w}_0'', \tag{28}$$

where M^h is zero for a zero applied higher-order moment. The displacement boundary conditions are

$$w_0 = \bar{w}_{0,} \quad w_0' = \bar{w}_0', \quad w_0'' = \bar{w}_0'' \tag{29}$$

at the fixed end. They are

$$w_0 = \bar{w}_{0,} \quad M - \frac{\partial M^h}{\partial x} = \bar{M}, \quad M^h = 0 \tag{30}$$

at the simply supported end; and they are

$$Q = \frac{\partial M}{\partial x} - \frac{\partial^2 M^h}{\partial x^2} = \bar{Q}; \quad M - \frac{\partial M^h}{\partial x} = \bar{M}, \quad M^h = \bar{M}^h \tag{31}$$

at the free end.

3.4 Relaxation and Creep of Simple Maxwell Materials

In the subsequent discussion, we shall consider the relaxation and creep problems with the inertia effect neglected.

$$-D_0D_1(t)\frac{\partial^4 w_0}{\partial x^4}+D_0[D_3(t)-D_2(t)]\frac{\partial^6 w_0}{\partial x^6}=0 \tag{32}$$

For a cantilever beam clamped at $x=0$, the boundary conditions [assuming $M^h(0,t)=M^h(l,t)=0$] are

$$w_0(0,t)=w_0'(0,t)=w_0'''(0,t)=-D_1\frac{\partial^2 w_0}{\partial x^2}(l,t)+D_L\frac{\partial^4 w_0}{\partial x^4}(l,t)=w_0'''(l,t)=0 \tag{33}$$

$$w_0(l,t)=w_0(l) \tag{34}$$

for relaxation problems; and

$$-D_0[D_1\frac{\partial^3 w_0}{\partial x^3}(l,t)-D_L\frac{\partial^5 w_0}{\partial x^5}(l,t)]=\bar{Q} \tag{35}$$

for creep.

For conventional simple Maxwell materials, there are two parallel springs, one with a series damper and one without, associated with the strains. We call them the first and second springs, respectively. We have

$$P_3(\frac{\partial}{\partial t})=1+\eta\frac{\partial}{\partial t},\quad Q_3(\frac{\partial}{\partial t})=\mu[1+\eta(1+\frac{\mu_1}{\mu})\frac{\partial}{\partial t}], \tag{36}$$

where μ and μ_1 are the first and second spring constants (shear moduli), and $\mu_1\eta$ is the viscosity coefficient of the damper in series with the second spring. For materials with strain gradient effects, we assume a separate, but similar, spring set for the strain gradients, *i.e.*,

$$\begin{aligned}&P_0\frac{\partial}{\partial t}=P_1\frac{\partial}{\partial t}=P_2\frac{\partial}{\partial t}=1+\eta\frac{\partial}{\partial t};\\&Q_0\frac{\partial}{\partial t}=Q_1\frac{\partial}{\partial t}=Q_2\frac{\partial}{\partial t}=\mu_g\left[1+\eta\left(1+\frac{\mu_{1h}}{\mu_h}\right)\frac{\partial}{\partial t}\right]\end{aligned} \tag{37}$$

Here, to simplify the solution, we have assumed that the viscosity coefficient of the second strain gradient spring is $\mu_{1h}\eta$. In this case, we have

$$\begin{aligned}&P_0\frac{\partial}{\partial t}=P_1\frac{\partial}{\partial t}=P_2\frac{\partial}{\partial t}=1+\eta\frac{\partial}{\partial t};\\&Q_0\frac{\partial}{\partial t}=Q_1\frac{\partial}{\partial t}=Q_2\frac{\partial}{\partial t}=\mu_g\left[1+\eta\left(1+\frac{\mu_{1h}}{\mu_h}\right)\frac{\partial}{\partial t}\right]\end{aligned} \tag{38}$$

in which

$$G_0 = D_0(1 + \frac{b_h^2}{h^2}\frac{\mu_{0h}}{\mu}), \qquad G_1 = D_0\frac{\mu_1}{\mu}(1 + \frac{b_h^2}{h^2}\frac{\mu_{1h}}{\mu_1})$$
$$G_{0h} = D_0(1 + \frac{\beta_h^2}{h^2}\frac{\mu_{0h}}{\mu}), \qquad G_{1h} = D_0\frac{\mu_1}{\mu}(1 + \frac{\beta_h^2}{h^2}\frac{\mu_{1h}}{\mu_1}) \tag{39}$$

With

$$\beta_h^2 = \left(\frac{11}{3} - \frac{26\nu}{3} - 2\nu^2\right)\frac{l_1^2}{1-\nu} - \frac{5(1+\nu)(1-2\nu)}{1-\nu}l_0^2 - \frac{5}{2}l_2^2 \tag{40}$$

depend on the material length scale parameters.

We further assume that

$$\frac{\mu_{0h}}{\mu} = \frac{\mu_{1h}}{\mu_1}. \tag{41}$$

Then we have

$$\frac{G_1}{G_0} = \frac{G_{1h}}{G_{0h}} = \frac{\mu_1}{\mu}. \tag{42}$$

Equation (32) reduces to

$$-G_0[1 + \eta(1 + \frac{\mu_1}{\mu})\frac{\partial}{\partial t}](\frac{\partial^4 w_0}{\partial x^4} - \frac{h^2}{20}G_{0h}\frac{\partial^6 w_0}{\partial x^6}) = 0. \tag{43}$$

The corresponding moment and shear force equilibrium equations are

$$(1 + \eta\frac{\partial}{\partial t})(M - \frac{\partial M_h}{\partial x}) = -G_0[1 + \eta(1 + \frac{\mu_1}{\mu})\frac{\partial}{\partial t}](\frac{\partial^2 w_0}{\partial x^2} - \frac{h^2}{20}\frac{G_{0h}}{G_0}\frac{\partial^4 w_0}{\partial x^4})$$
$$(1 + \eta\frac{\partial}{\partial t})Q = -G_0[1 + \eta(1 + \frac{\mu_1}{\mu})\frac{\partial}{\partial t}](\frac{\partial^3 w_0}{\partial x^3} - \frac{h^2}{20}\frac{G_{0h}}{G_0}\frac{\partial^5 w_0}{\partial x^5}). \tag{44}$$

The fourth boundary condition of Eq. (33) can be written as

$$[1 + \eta(1 + \frac{\mu_1}{\mu})\frac{\partial}{\partial t}] \cdot [G_0\frac{\partial^2 w_0(l,t)}{\partial x^2} - \frac{h^2}{20}G_{0h}\frac{\partial^4 w_0(l,t)}{\partial x^4}] = 0. \tag{45}$$

3.4.1 Relaxation

For relaxation, the deflection, w_0, is given in Eq. (E1), which is the solution of Eq. (43) with the boundary conditions Eqs. (33) and (35). The deflection is independent of t. The shear force, given in Eq.(E6), is derived from Eq. (45) with the initial condition at $t = 0$,

$$Q = -(G_0 + G_1)\left(\frac{\partial^3 w_0}{\partial x^3} - \frac{h^2}{20}\frac{G_{0h}}{G_0}\frac{\partial^5 w_0}{\partial x^5}\right). \tag{46}$$

If we neglect the term proportional to h^2 for thin beams in Eq. (43), the deflection given in Eq. (E1) reduces to

$$w_0(x,t) = \frac{3}{2}\frac{x^2}{l^2}(1 - \frac{1}{3}\frac{x}{l})w_0(l). \tag{47}$$

Solving the moment and shear force equations

$$(1+\eta\frac{\partial}{\partial t})M = -G_0\frac{d^2 w_0}{dx^2}; \quad (1+\eta\frac{\partial}{\partial t})Q = -G_0\frac{d^3 w_0}{dx^3} \tag{48}$$

gives

$$M(x,t) = -G_0\left(1 + \frac{\mu_1}{\mu}e^{-t/\eta}\right)\frac{3}{l^2}\left(1 - \frac{x}{l}\right)w_0(l) \tag{49}$$

$$Q = \frac{\partial M}{\partial x}(x,t) = \frac{3}{l^3}G_0\left(1 + \frac{\mu_1}{\mu}e^{-t/\eta}\right)w_0(l) \tag{50}$$

It is of interest to note that there is no size dependence in the exponentially decaying time function in relaxation of simple Maxwell materials that satisfy Eq. (35).

3.4.2 Creep

For creep, the transversal shear force and the moment are independent of time such that

$$Q(x,t) = \bar{Q}; \quad M(x,t) = (x-l)\bar{Q}, \tag{51}$$

where $\bar{Q}$ is the applied shear force at the free end. The deflection, w_0, is in the same form as Eq. (E1) in which $w_0(l,t)$ is now a function of time. The initial condition for $w_0(l,t)$ is similar to Eq. (46) with Q replaced by $\bar{Q}$.

The solution is given in Eq. (E8), which is the creep relation between the deflection and the applied shear force at the tip of the beam.

If the term proportional to h^2 in Eq. (43) is neglected for thin beams, the creep relation reduces to

$$w_0(l,t) = \frac{l^3\bar{Q}}{3G_0}\left[1 - \frac{\mu_1}{\mu+\mu_1}e^{-\frac{\mu}{\mu+\mu_1}\frac{t}{\eta}}\right]. \tag{52}$$

Similar to relaxation, there is no size dependence in the exponentially decaying time function when simple Maxwell materials that satisfy Eq. (41) creep.

3.5 Simple Kelvin-Voigt Materials

For conventional simple Kelvin-Voigt materials, there are two springs in series, one of which has a parallel damper and one has no parallel damper, associated with the strains. We have

$$Q_3\frac{\partial}{\partial t}/P_3\frac{\partial}{\partial t} = \mu\mu_1\left(1+\eta\frac{\partial}{\partial t}\right)\left[\mu+\mu_1\left(1+\eta\frac{\partial}{\partial t}\right)\right]^{-1} \tag{53}$$

where μ and μ_1 are the first and second spring constants (shear moduli), and $\mu_1\eta$ is the viscosity coefficient of the damper in series with the second spring. For materials with strain gradient effects, we assume a separate, but similar, spring set for the strain gradients, *i.e.*,

$$Q_j\frac{\partial}{\partial t}/P_j\frac{\partial}{\partial t} = \mu_{0h}\mu_{1h}\left(1+\eta\frac{\partial}{\partial t}\right)\left[\mu_{0h}+\mu_{1h}\left(1+\eta\frac{\partial}{\partial t}\right)\right]^{-1} \tag{54}$$

for j = 0, 1, and 2. As before, we have assumed that the viscosity coefficient of the strain gradient spring with a damper is $\mu_{1h}\eta$.

With materials satisfying Eq. (41), Eq. (32) reduces to

$$-(1+\eta D)(G_0\frac{\partial^4 w_0}{\partial x^4} - \frac{h^2}{20}G_{0h}\frac{\partial^6 w_0}{\partial x^6}) = 0. \tag{55}$$

The corresponding moment and shear force equilibrium equations are

$$(1+\frac{\mu}{\mu_1}+\eta D)(M-\frac{\partial M_h}{\partial x}) = -(1+\eta D)(G_0\frac{\partial^2 w_0}{\partial x^2} - \frac{h^2}{20}G_{0h}\frac{\partial^4 w_0}{\partial x^4}), \tag{56}$$

$$(1+\frac{\mu}{\mu_1}+\eta D)Q = -(1+\eta D)(G_0\frac{\partial^3 w_0}{\partial x^3} - \frac{h^2}{20}G_{0h}\frac{\partial^5 w_0}{\partial x^5}). \tag{57}$$

For both relaxation and creep, the deflection w_0 is in the form of Eq. (E1). The initial condition at t = 0 for the Kelvin-Voigt model is

$$Q = -(G_0\frac{\partial^3 w_0}{\partial x^3} - \frac{h^2}{20}G_{0h}\frac{\partial^5 w_0}{\partial x^5}) \tag{58}$$

in which w_0 is independent of t for relaxation while $Q(=\bar{Q})$ is independent of t for creep. The fourth boundary condition of Eq. (33) can be written as

$$(1+\eta\frac{\partial}{\partial t})[G_0\frac{\partial^2 w_0(l,t)}{\partial x^2}-\frac{h^2}{20}G_{0h}\frac{\partial^4 w_0(l,t)}{\partial x^4}]=0. \tag{59}$$

3.5.1 Relaxation

For a sudden deflection of $w_0(l)$ at $x = l$, the solution that satisfies the boundary conditions of Eqs. (33) and (34) is the same as that given in Eq. (E1) with $w_0(l,t) = w_0(l)$. From Eq.(57), we determine the solution for Q as given in Eq.(F3).

If we neglect the term proportional to h^2 for thin beams in Eq.(43), the deflection is the same as that given in Eq.(47). The relaxation relation reduces to

$$Q=\frac{\partial M}{\partial x}(x,t)=\frac{3}{l^3}G_0[1+\frac{\mu}{\mu_1}\exp(-\frac{\mu+\mu_1}{\mu_1}\frac{t}{\eta})]w_0(l). \tag{60}$$

Similar to Maxwell materials, there is no size dependence in the exponentially decaying time function in the relaxation of simple Kelvin-Voigt materials satisfying Eq.(41).

3.5.2 Creep

For a sudden applied shear force, $\bar{Q}$, at $x = l$, the solution that satisfies the boundary conditions, Eqs. (33) and (34), is the same as that given in Eq.(47). Equation (57) gives the creep relation between the tip deflection and the applied shear force as shown in Eq. (F5).

Again, if the term proportional to h^2 in Eq. (43) is neglected in thin beams, the creep relation reduces to

$$w_0(l,t)=\frac{l^3\bar{Q}}{3G_0}[1+\frac{\mu}{\mu_1}-\frac{\mu}{\mu_1}\exp(-\frac{t}{\eta})], \tag{61}$$

and after substitution of variables, we have

$$\frac{w_0(l,t)}{2\bar{Q}\frac{l^3}{h^3}}\left(1-\nu+\frac{3l_2^2}{h^2}\right)=\frac{1}{\mu_0}+\frac{1}{\mu_1}-\frac{1}{\mu_1}\exp\left(-\frac{\mu_1 t}{\eta_1}\right). \tag{62}$$

As for relaxation, creep has no size dependence in the exponentially decaying time function for simple Kelvin-Voigt materials that satisfy Eq. (41).

4 Experiments

Epoxy beams made from a mixture of Bisphenol-A epichlorohydrin resin and 20 phr of diethylenetriamine hardener were fabricated. The beam thicknesses were controlled by spin casting the degassed epoxy onto low-adhesion glass plates with spacers (between 20 – 300 μm) to control the gap size. The cast sandwich assemblies were cured at 100^{o}C for 3 hours and cooled slowly to room temperature following a previously established procedure (Lam and Chong, 1999). The glass plates were then removed from the cured epoxy plates. Identical parallel cuts were made on the beams to form identical rows of cantilever beams and adhesively mounted onto glass substrates. The beams were loaded at lengths between 20 to 40 multiples (l/h) of the beam thicknesses to minimize the anchor effects. The loads were applied using a nanoindentor (Hysitron Triboindentor) fitted with a pyramidal Berkovich tip. The nanoindentor had a load resolution from 100 nN with a displacement resolution under 1 nm. In our experiments, beams were deflected up to 1000 nm for applied loads between 20 to 60 μN. The local indentation effects on the overall deflection were small and were ignored.

5 Results

The deflection behavior of the epoxy beams was checked to ensure that they were Kelvin-Voigt viscoelastic beams. The creep deflection from a representative test is shown in Figure 1. Agreement between the experimental data and the model (Figure 1) confirmed that the tested beams were Kelvin-Voigt viscoelastic beams. The deflection curves for beams with different thicknesses loaded at $l/h = 20$ and $\overline{Q}$=30μN are shown in Figure 2. If the deflection behaved classically without added size-dependence, the curves at identical l/h would collapse onto a single curve. Instead, the thin beams have lower normalized deflections than the thick beams have in Figure 2. A close-up plot (Figure 3) shows that the slope of the deflection in the initial elastic regime also has an inverse dependence on the beam thickness. This suggests that the beam stiffness in Figure 2 has an added inverse dependence on the beam thickness in both the elastic and time-dependent regimes.

The thickness dependence is eliminated after the deflections are normalized (Figure 4) using l_2 = 34 μm. The plot showed that the initial fast-rising portion of the deflection where $\mu_{0,rg}$ dominated, i.e., the elastic portion, has collapsed. The creeping portion in the second stage has also collapsed onto a single curve with the same l_2. In fact, all curves from start to finish collapsed onto a single curve (Figure 5) using the same l_2 for all beam thicknesses in the elastic and the creeping regimes. The collapse confirmed that the constants, $\mu_{0,rg}$, $\mu_{1,rg,}$and$\eta_{1,rg}$, have the same the thickness and l_2 dependence.

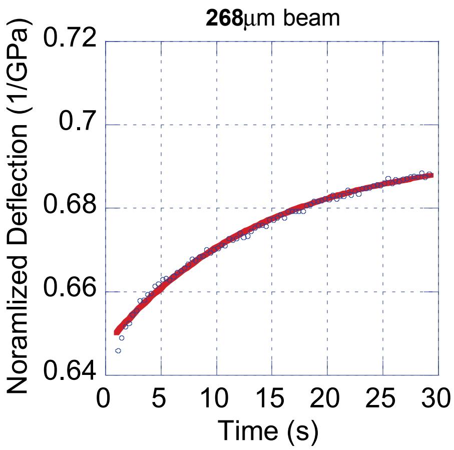

Figure 1: A normalized creep deflection curve for a 268 micron thick beam co-plotted with a conventional Voigt model (solid curve).

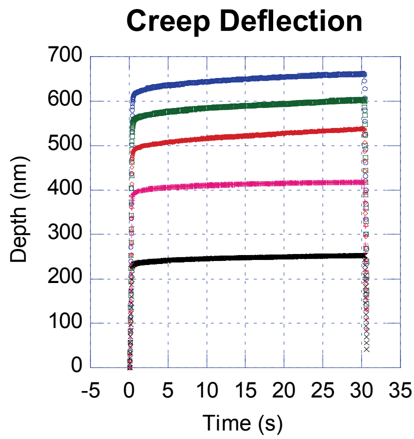

Figure 2: Creep deflection in relation to thicknesses from 26 (top curve), 39, 65, 135 and 268 microns (bottom curve) at constant $l/h = 20$.

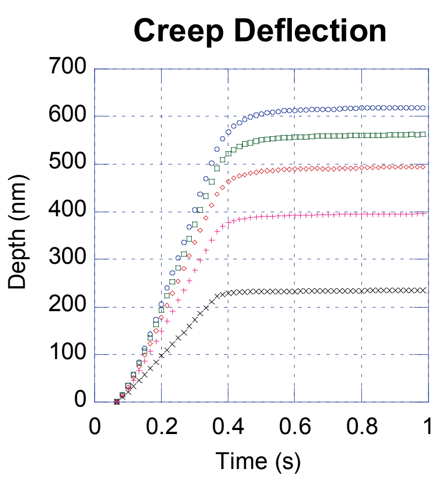

Figure 3: A close-up view of the elastic regime before reaching the set load for creep.

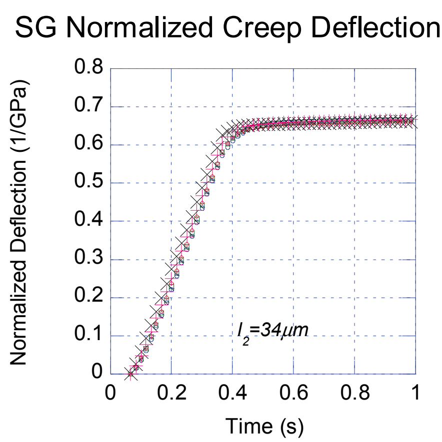

Figure 4: Normalized deflection using l^2=34 microns.

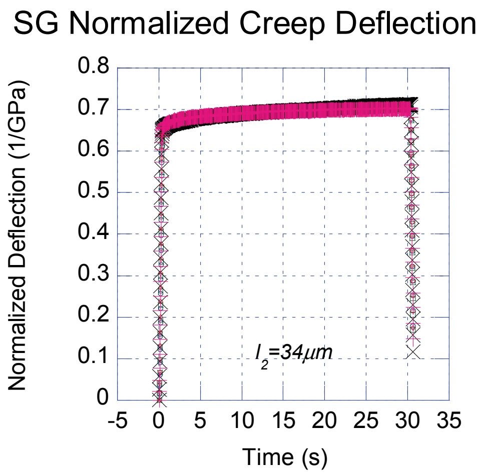

Figure 5: A deflection curve normalized using l_2=34 microns.

6 Discussion

In Part I of this series, molecular rotation is identified as the underlying deformation mechanism for $l_{2,}$ and that it shares the same deformation mechanism as the strain-based elastic deformation. Moreover, it is a parameter characterizing the extended association of the deformation mechanism from strain to rotation gradients. The single l_2 results ascertained in this investigation is a natural consequence of this extension view of l_2.

In the viscoelastic regime, the deformation behavior of the macromolecular solid is characterized by multiple material constants, i.e., μ_0, μ_1, and η_1. If l_2 is tied to specific material constants, then there would be different l_2 for each spring and dashpot constant since each maybe tied to their respective effects, which can include alignment (Fleck et al., 1994), surface (Cuenot, Frétigny, and Demoustier-Champagne, 2004) or the supramolecular effects (Arinstein, Burman, and Gendelman, 2007). Instead, this study showed that $\mu_{0,rg}$, $\mu_{1,rg,}$and $\eta_{1,rg}$ have identical l_2. This suggests that l_2 is not tied specifically to a physical mechanism, but is a characteristic multiplier of rotation gradient deformations. In other words, the relationship between strain (or strain rate) and stress for a specific mechanism is already characterized by its set of material constants, and the relationship is simply extended to rotation gradients (or gradient rates) by l_2. The extension is a new association, and not a new mechanism. The association is fundamentally chain-based and is not deformation mechanism-based. Since there is only one set of chains within a single solid, there is only one l_2 for the solid. l_2 is unique to the chemistry and the molecular structure of the chain, and is not unique to the deformation regime of the solid.

7 Conclusions

Molecular rotation was identified as the deformation mechanism behind higher-order elastic deformation of macromolecular solid. Higher-order viscoelasticity framework and creep bending models were developed based on the hypothesis that the elastic and viscous material constants shared the same higher order material constant. Experimental results from creep tests on macromolecular beams in this study showed that a single chain-based l_2 controlled both the elastic and viscoelastic higher-order deformation of macromolecular polymers. This means that irrespective of the number of springs and dashpots in the strain-based phemenological constitutive law, only a single l_2 is required to transform strain- and strain rate-based viscoelastic law into higher order viscoelastic constitutive law for macromolecular solids.

Appendix A Summary of strain gradient theory for linear elasticity

In the strain gradient elasticity theory, the second-order deformation gradient tensors are the dilatation gradient vector, γ_i, the deviatoric stretch gradient tensor, η_{ijk}, and the symmetric rotational gradient (curvature) tensor, χ_{ij}. These strain measures are defined as

$$\varepsilon_{ij} = \frac{1}{2}(\partial_i u_j + \partial_j u_i), \quad \gamma_i = \partial_i \varepsilon_{mm},$$

$$\eta_{ijk} = \frac{1}{3}(\partial_i \varepsilon_{jk} + \partial_j \varepsilon_{ki} + \partial_k \varepsilon_{ij}) - \frac{1}{15}\left[\delta_{ij}(\partial_k \varepsilon_{mm} + 2\partial_m \varepsilon_{mk}) + \delta_{jk}(\partial_i \varepsilon_{mm} + 2\partial_m \varepsilon_{mi}) + \delta_{ki}(\partial_j \varepsilon_{mm} + 2\partial_m \varepsilon_{mj})\right],$$

$$\chi_{ij} = \frac{1}{2}(e_{ipq}\partial_p \varepsilon_{qj} + e_{jpq}\partial_p \varepsilon_{qi}), \tag{A1}$$

where ∂_i is the forward gradient operator, u_i the displacement vector, δ_{ij} the Kronecker delta and e_{ijk} the alternating tensor; and ε_{ij} is the strain tensor with six independent symmetric components. There are three independent components in γ_i, seven in η_{ijk}, and five in χ_{ij} mean that there is a total of 15 independent components in the second-order deformation gradient tensors. The stress measures, the work-conjugates to the strain measures, are the classical stress tensor, $\sigma_{ij,}$ and the higher-order stresses, p_i, τ_{ijk} and m_{ij}.

For linear elastic center-symmetric isotropic materials, the constitutive relations are

$$\sigma_{ij} = \lambda \delta_{ij} \varepsilon_{mm} + 2\mu \varepsilon_{ij} \quad p_i = 2\mu l_0^2 \varepsilon_{mm,i}, \quad \tau_{ijk} = 2\mu l_1^2 \eta_{ijk}, \quad m_{ij} = 2\mu l_2^2 \chi_{ij}, \tag{A2}$$

where λ and μ are Lame's constant and the shear modulus, respectively, and l_n (n= 0,1,2) are the three additional length scale material parameters associated with the dilatation, deviatoric stretch and rotation gradients, respectively.

Appendix B Linear Isotropic Viscoelasticity in Convolution Integral Form

The constitutive relations for linear isotropic viscoelastic materials in convolution integral form are

$$\sigma_{ij}(\mathbf{x},t) = \int_{-\infty}^{t} \lambda(\mathbf{x}, t-\tau) \delta_{ij} \frac{\partial \varepsilon_{mm}(\mathbf{x},\tau)}{\partial \tau} d\tau + 2\int_{-\infty}^{t} \mu(\mathbf{x}, t-\tau) \frac{\partial \varepsilon_{ij}(\mathbf{x},\tau)}{\partial \tau} d\tau, \tag{B1}$$

$$p_i(\mathbf{x},\tau) = 2l_0^2 \int_{-\infty}^{t} \mu_0(\mathbf{x}, t-\tau) \frac{\partial \varepsilon_{mm,i}(\mathbf{x},\tau)}{\partial \tau} d\tau, \tag{B2}$$

$$\tau_{ijk} = 2l_1^2 \int_{-\infty}^{t} \mu_1(\mathbf{x}, t-\tau) \frac{\partial \eta_{ijk}(\mathbf{x},\tau)}{\partial \tau} d\tau, \tag{B3}$$

$$m_{ij} = 2l_2^2 \int_{-\infty}^{t} \mu_2(\mathbf{x}, t-\tau) \frac{\partial \chi_{ij}(\mathbf{x},\tau)}{\partial \tau} d\tau, \tag{B4}$$

where λ and the μ are relaxation functions. A simple viscoelastic model is

$$\lambda(\mathbf{x},\tau) = \frac{2\nu}{1-2\nu} \mu(\mathbf{x},\tau), \tag{B5}$$

$$\mu_0(\mathbf{x},\tau) = \mu_1(\mathbf{x},\tau) = \mu_2(\mathbf{x},\tau), \tag{B6}$$

in which the Poisson ratio, ν, is independent of time.

Appendix C General Equilibrium Equations

The general equilibrium equations along the directions of length and thickness of the beam are

$$\begin{aligned} &\partial_1 (\sigma_{11} - \partial_1 p_1 - \partial_1 \tau_{111}) \\ &+ \partial_3 \left(\sigma_{13} - \frac{1}{2}\partial_1 m_{12} - \partial_1 p_3 - 2\partial_1 \tau_{113} - \frac{1}{2}\partial_3 m_{32} - \partial_3 \tau_{133} \right) = \rho \frac{\partial^2 u}{\partial t^2}, \\ &\partial_3 \left(\sigma_{33} + \frac{1}{2}\partial_1 m_{32} - \partial_1 p_1 - 2\partial_1 \tau_{133} - \partial_3 p_3 - \partial_3 \tau_{333} \right) \\ &+ \partial_1 \left(\sigma_{13} + \frac{1}{2}\partial_1 m_{12} - \partial_1 \tau_{113} \right) = \rho \frac{\partial^2 w}{\partial t^2}. \end{aligned} \tag{C1}$$

The traction-prescribed boundary conditions on the top and bottom surfaces of the beam are

$$\sigma_{33} - \partial_1 p_1 - \partial_3 p_3 - 3\partial_1 \tau_{133} - \partial_3 \tau_{333} = \bar{q}_{\pm h/2}, \tag{C2}$$

$$\sigma_{13} - \frac{1}{2}\partial_1 m_{12} - \partial_1 p_3 - 2\partial_1 \tau_{113} - \frac{1}{2}\partial_3 m_{32} - \partial_3 \tau_{133} = 0, \quad \forall z = \pm\frac{h}{2},$$

$$m_{32} + 2\tau_{133} = 0, \quad p_3 - \tau_{333} = 0, \tag{C3}$$

where $\bar{q}_{\pm h/2}$ is the prescribed normal force-traction on the top and bottom surfaces in units of N/m^2. The prescribed force-tractions on the surfaces normal to the $x-$axis and the boundary conditions at the edges of the top and bottom surfaces of the beam are given in Eqs. (57) and (58) of Lam *et al*. (2003).

Appendix D Bending Deformations and Constitutive Equations

For plain strain beams, the non-vanishing stresses and higher-order stresses are

$$\begin{aligned}
\sigma_{11} &= 2Q_c(\frac{\partial}{\partial t})\sum_{i=0}^{\infty}\left[\frac{1-\nu}{1-2\nu}\frac{\partial u_i}{\partial x} + \frac{\nu}{1-2\nu}\frac{\partial w_{i+1}}{\partial s}\right]h^i \\
\sigma_{33} &= 2Q_c(\frac{\partial}{\partial t})\sum_{i=0}^{\infty}\left[\frac{1-\nu}{1-2\nu}\frac{\partial w_{i+1}}{\partial s} + \frac{\nu}{1-2\nu}\frac{\partial u_i}{\partial x}\right]h^i \\
\sigma_{13} &= Q_c(\frac{\partial}{\partial t})\sum_{i=0}^{\infty}\left[\frac{\partial w_i}{\partial x} + \frac{\partial u_{i+1}}{\partial s}\right]h^i \\
\sigma_{22} &= \gamma(\sigma_{11} + \sigma_{33})
\end{aligned} \tag{D1}$$

$$\begin{aligned}
p_1 &= l_0^2 Q_g(\frac{\partial}{\partial t})\sum_{i=0}^{\infty}\frac{\partial}{\partial x}\left[\frac{\partial u_i}{\partial x} + \frac{\partial w_{i+1}}{\partial s}\right]h^i \\
p_3 &= l_0^2 Q_g(\frac{\partial}{\partial t})\sum_{i=0}^{\infty}\frac{\partial}{\partial s}\left[\frac{\partial u_{i+1}}{\partial x} + \frac{\partial w_{i+2}}{\partial s}\right]h^i
\end{aligned} \tag{D2}$$

$$\begin{aligned}
m_{21} &= -\frac{l_2^2}{4} Q_g(\frac{\partial}{\partial t})\sum_{i=0}^{\infty}\frac{\partial}{\partial x}\left[\frac{\partial w_i}{\partial x} - \frac{\partial u_{i+1}}{\partial s}\right]h^i \\
m_{23} &= -\frac{l_2^2}{4} Q_g(\frac{\partial}{\partial t})\sum_{i=0}^{\infty}\frac{\partial}{\partial s}\left[\frac{\partial w_{i+1}}{\partial x} - \frac{\partial u_{i+2}}{\partial s}\right]h^i
\end{aligned} \tag{D3}$$

and

$$\begin{aligned}
\tau_{111} &= l_1^2 Q_g(\frac{\partial}{\partial t})\cdot\sum_{i=0}^{\infty}\left[\frac{\partial}{\partial x}\left(\frac{2}{5}\frac{\partial u_i}{\partial x}-\frac{2}{5}\frac{\partial w_{i+1}}{\partial s}\right)-\frac{1}{5}\frac{\partial^2 u_{i+2}}{\partial s^2}\right]h^i;\\
\tau_{113} &= l_1^2 Q_g(\frac{\partial}{\partial t})\cdot\sum_{i=0}^{\infty}\left[\frac{\partial}{\partial x}\left(\frac{4}{15}\frac{\partial w_i}{\partial x}+\frac{8}{15}\frac{\partial u_{i+1}}{\partial s}\right)-\frac{1}{5}\frac{\partial^2 w_{i+2}}{\partial s^2}\right]h^i;\\
\tau_{133} &= -l_1^2 Q_g(\frac{\partial}{\partial t})\cdot\sum_{i=0}^{\infty}\left[\frac{\partial}{\partial x}\left(\frac{1}{5}\frac{\partial u_i}{\partial x}-\frac{8}{15}\frac{\partial w_{i+1}}{\partial s}\right)-\frac{4}{15}\frac{\partial^2 u_{i+2}}{\partial s^2}\right]h^i;\\
\tau_{333} &= -l_1^2 Q_g(\frac{\partial}{\partial t})\cdot\sum_{i=0}^{\infty}\left[\frac{\partial}{\partial x}\left(\frac{1}{5}\frac{\partial w_i}{\partial x}+\frac{2}{5}\frac{\partial u_{i+1}}{\partial s}\right)-\frac{2}{5}\frac{\partial^2 w_{i+2}}{\partial s^2}\right]h^i;\\
\tau_{122} &= -(\tau_{111}+\tau_{133}),\quad \tau_{223}=-(\tau_{133}+\tau_{333}),
\end{aligned}\tag{D4}$$

where

$$\begin{aligned}
&Q_c(\frac{\partial}{\partial t}) = Q_3(\frac{\partial}{\partial t})/P_3(\frac{\partial}{\partial t}),\\
&Q_g(\frac{\partial}{\partial t}) = Q_3(\frac{\partial}{\partial t})/P_3(\frac{\partial}{\partial t}) = Q_0(\frac{\partial}{\partial t})/P_0(\frac{\partial}{\partial t}) = Q_2(\frac{\partial}{\partial t})/P_2(\frac{\partial}{\partial t}),
\end{aligned}\tag{D5}$$

for $P_0 = P_1 = P_2$ and $Q_0 = Q_1 = Q_2$.

The expansion of the second boundary equation in Eq. (C2) gives the $O(h^i)$ equation:

$$\begin{aligned}
&Q_c\frac{\partial}{\partial t}\left(\frac{\partial w_i}{\partial x}+\frac{\partial u_{i+1}}{\partial s}\right)\\
&+Q_g\frac{\partial}{\partial t}\left[\left(\frac{l_2^2}{8}-\frac{8l_1^2}{15}\right)\frac{\partial^3 w_i}{\partial x^3}+\left(\frac{2l_1^2}{5}-l_0^2\right)\frac{\partial^3 w_{i+2}}{\partial x\partial s^2}-\left(\frac{l_2^2}{8}+\frac{16l_1^2}{15}+l_0^2\right)\frac{\partial^3 u_{i+1}}{\partial x^2\partial s}\right]\\
&=0,
\end{aligned}\tag{D6}$$

where $i = 0,1,2,\ldots$. Similarly from the first and second equilibrium equations, Eq.(C1), we obtain, respectively,

$$\begin{aligned}
&Q_c\frac{\partial}{\partial t}\left[\frac{2(1-\nu)}{1-2\nu}\frac{\partial^2 u_i}{\partial x^2}+\frac{1}{1-2\nu}\frac{\partial^2 w_{i+1}}{\partial x\partial s}+\frac{\partial^2 u_{i+2}}{\partial s^2}\right]\\
&+Q_g\frac{\partial}{\partial t}\left[-\left(-\frac{2l_1^2}{5}+l_0^2\right)\frac{\partial^4 u_i}{\partial x^4}+\left(\frac{l_2^2}{8}-\frac{2l_1^2}{15}-l_0^2\right)\left(\frac{\partial^4 w_{i+1}}{\partial x^3\partial s}+\frac{\partial^4 w_{i+3}}{\partial x\partial s^3}\right)\right.\\
&\qquad\left.-\left(\frac{l_2^2}{8}+\frac{2l_1^2}{3}+l_0^2\right)\frac{\partial^4 u_{i+2}}{\partial x^2\partial s^2}-\left(\frac{l_2^2}{8}+\frac{4l_0^2}{15}\right)\frac{\partial^4 u_{i+4}}{\partial s^4}\right]=0,
\end{aligned}\tag{D7}$$

$$
\begin{aligned}
&Q_c\frac{\partial}{\partial t}\left[\frac{\partial^2 w_i}{\partial x^2}+\frac{1}{1-2\nu}\frac{\partial^2 u_{i+1}}{\partial x\partial s}+\frac{2(1-\nu)}{1-2\nu}\frac{\partial^2 u_{i+2}}{\partial s^2}\right]\\
&+Q_g\frac{\partial}{\partial t}\left[-\left(\frac{l_1^2}{8}+\frac{4l_1^2}{15}\right)\frac{\partial^4 w_i}{\partial x^4}+\left(\frac{l_2^2}{8}-\frac{2l_1^2}{15}-l_0^2\right)\frac{\partial^4 u_{i+1}}{\partial x^3\partial s}\right.\\
&\left.-\left(\frac{l_2^2}{8}+\frac{2l_1^2}{3}+l_0^2\right)\frac{\partial^4 w_{i+2}}{\partial x^2\partial s^2}+\left(\frac{l_2^2}{8}-\frac{2l_0^2}{15}-l_0^2\right)\frac{\partial^4 u_{i+3}}{\partial x\partial s^3}-\left(\frac{l_2^2}{5}+l_0^2\right)\frac{\partial^4 w_{i+4}}{\partial s^4}\right]=0,
\end{aligned}
\tag{D8}
$$

with the assumption that the inertia force is small and can be neglected. First, from Eqs. (D7) and (D8), we can express $u_3, u_5, \ldots$ and $w_2, w_4, \ldots$ in terms of w_0, u_1, and $u_2, u_4, \ldots$ and $w_3, w_5, \ldots$ in terms of u_0, w_1 and their derivatives. Then, together with the O(1) equation of Eq.(D6), we determine u_1 in terms of w_0 and w_1 in terms of u_0 and the respective partial derivative with respect to x. In turn, we obtain $u_3, u_5, \ldots$ and $w_2, w_4, \ldots$ in terms of w_0 and the partial derivatives with respect to x and $u_2, u_4, \ldots$ and $w_1, w_3, \ldots$ in terms of u_0 and its partial derivatives. The results are as follows:

$$
\begin{aligned}
Q_c(\frac{\partial}{\partial t})\frac{\partial^2 w_4}{\partial s^2}&=-\frac{1-2\nu}{2(1-\nu)}Q_c(\frac{\partial}{\partial t})[\frac{\partial^2 w_2}{\partial x^2}+\frac{1}{1-2\nu}\frac{\partial^2 u_3}{\partial x\partial s}]+O(l_0^2,l_1^2,l_2^2)\\
&=-\frac{s^2}{2}\frac{1+\nu}{1-\nu}Q_c(\frac{\partial}{\partial t})\frac{\partial^4 w_0}{\partial x^4}+O(l_0^2,l_1^2,l_2^2,h^2)
\end{aligned}
\tag{D9}
$$

$$
\begin{aligned}
&Q_c(\frac{\partial}{\partial t})\frac{\partial^2 u_3}{\partial s^2}=-Q_c(\frac{\partial}{\partial t})[\frac{2(1-\nu)}{1-2\nu}\frac{\partial^2 u_1}{\partial x^2}+\frac{1}{1-2\nu}\frac{\partial^2 w_2}{\partial x\partial s}]+O(l_0^4,l_1^4,l_2^4)\\
&=s\{\frac{2-\nu}{1-\nu}Q_c(\frac{\partial}{\partial t})\frac{\partial^3 w_0}{\partial x^3}+\frac{3-2\nu}{2(1-\nu)^2}[\frac{1-\nu}{4}l_2^2+\frac{2(4-\nu)}{15}l_1^2+(1-2\nu)l_0^2]\\
&\qquad Q_g(\frac{\partial}{\partial t})\frac{\partial^4 w_0}{\partial x^4}\}+O(l_0^4,l_1^4,l_2^4,h^2)
\end{aligned}
\tag{D10}
$$

$$
\begin{aligned}
&Q_c(\frac{\partial}{\partial t})\frac{\partial^2 w_2}{\partial s^2}=-\frac{1-2\nu}{2(1-\nu)}Q_c(\frac{\partial}{\partial t})[\frac{\partial^2 w_0}{\partial x^2}+\frac{1}{1-2\nu}\frac{\partial^2 u_1}{\partial x\partial s}]+O(l_0^4,l_1^4,l_2^4)\\
&=\frac{\nu}{1-\nu}Q_c(\frac{\partial}{\partial t})\frac{\partial^2 w_0}{\partial x^2}+\frac{1}{2(1-\nu)^2}[\frac{1-\nu}{4}l_2^2+\frac{2(4-\nu)}{15}l_1^2+(1-2\nu)l_0^2]\\
&\qquad Q_g(\frac{\partial}{\partial t})\frac{\partial^4 w_0}{\partial x^4}+O(l_0^4,l_1^4,l_2^4,h^4)
\end{aligned}
\tag{D11}
$$

$$
\begin{aligned}
&Q_c(\frac{\partial}{\partial t})\frac{\partial u_1}{\partial s} = -Q_c(\frac{\partial}{\partial t})\frac{\partial w_0}{\partial x} \\
&-Q_g(\frac{\partial}{\partial t})[(\frac{l_2^2}{8}-\frac{8l_1^2}{15})\frac{\partial^3 w_0}{\partial x^3}+(\frac{2l_1^2}{5}-l_0^2)\frac{\partial^3 w_2}{\partial x\partial s^2}-(\frac{l_2^2}{8}+\frac{16l_1^2}{15}+l_0^2)\frac{\partial^3 u_1}{\partial x^2\partial s}] \\
&= -Q_c(\frac{\partial}{\partial t})\frac{\partial w_0}{\partial x}-\frac{1}{1-\nu}[\frac{1-\nu}{4}l_2^2+\frac{2(4-\nu)}{15}l_1^2+(1-2\nu)l_0^2] \\
&\qquad Q_g(\frac{\partial}{\partial t})\frac{\partial^3 w_0}{\partial x^3}+O(l_0^4,l_1^4,l_2^4,h^4) \qquad \text{(D12)}
\end{aligned}
$$

In Eqs. (D11) and (D12), the inertia force associated with w_2 has been neglected. Similar results can be obtained for $u_2, u_4, \ldots$ and $w_3, w_5, \ldots$ in terms of u_0. For pure bending, the axial and higher-order axial stress resultants (Eq.(12)) vanish and give

$$u_0 = u_2 = \ldots = w_1 = w_3 = \ldots = 0. \qquad \text{(D13)}$$

For only bending, the curvature, κ, and the curvature gradient, κ_h, are, respectively

$$\kappa = -w_0''(x), \quad \kappa^h = -w_0'''(x). \qquad \text{(D14)}$$

By combining Eqs. (D1) – (D4) and (D9) – (D12), the constitutive equations for the non-vanishing stresses and higher-order stresses in terms of the curvature and the curvature gradients become

$$
\begin{aligned}
\sigma_{11} &= -\frac{2hs}{1-\nu}Q_c\frac{\partial}{\partial t}\left(\kappa-\frac{h^2s^2}{3}\frac{\partial\kappa^h}{\partial x}\right) \\
&-\left[\frac{1-\nu}{4}l_2^2+\frac{2(4-\nu)}{15}l_1^2+(1-2\nu)l_0^2\right]\frac{(2-\nu)hs}{(1-\nu)^2}Q_g\frac{\partial}{\partial t}\frac{\partial\kappa^h}{\partial x}+O(l_i^4mh^5) \qquad \text{(D15)}
\end{aligned}
$$

$$
\begin{aligned}
&p_1 = -\frac{1-2\nu}{1-\nu}hsl_0^2Q_g(\frac{\partial}{\partial t})\kappa^h+O(l_0^2h^3) \\
&p_3\frac{1-2\nu}{1-\nu}l_0^2Q_g(\frac{\partial}{\partial t})(-\kappa+\frac{h^2s^2}{2}\frac{\partial\kappa^h}{\partial x})+O(l_0^2h^4)
\end{aligned} \qquad \text{(D16)}
$$

$$
\begin{aligned}
&\tau_{111} = -\frac{4-\nu}{5(1-\nu)}hsl_1^2Q_g(\frac{\partial}{\partial t})\kappa^h+O(l_1^2h^3) \\
&\tau_{113} = -l_1^2Q_g(\frac{\partial}{\partial t})[\frac{4-\nu}{15(1-\nu)}\kappa-\frac{19-\nu}{30(1-\nu)}h^2s^2\frac{\partial\kappa^h}{\partial x}]+O(l_1^2h^4) \\
&\tau_{133} = -\frac{11+\nu}{15(1-\nu)}hsl_1^2Q_g(\frac{\partial}{\partial t})\kappa^h+O(l_1^2h^3) \\
&\tau_{333} = l_1^2Q_g(\frac{\partial}{\partial t})[\frac{1+\nu}{5(1-\nu)}\kappa-\frac{\nu+6}{10(1-\nu)}h^2s^2\frac{\partial\kappa^h}{\partial x}]+O(l_1^2h^4)
\end{aligned} \qquad \text{(D17)}
$$

$$
\begin{aligned}
m_{12} &= -l_2^2 Q_g(\frac{\partial}{\partial t})[\frac{\kappa}{2} - \frac{h^2 s^2}{4}\frac{\partial \kappa^h}{\partial x}] + O(l_2^2 h^4) \\
m_{32} &= hsl_2^2 Q_g(\frac{\partial}{\partial t})[\frac{\kappa}{2} - \frac{h^2 s^2}{12}\frac{\partial \kappa^h}{\partial x}] + O(l_2^2 h^4)
\end{aligned} \tag{D18}
$$

After solving the bending problem, the stresses and higher-order stresses can be obtained from Eqs. (D4) – (D7). The exception is that σ_{13} and σ_{33} should be determined by integrating Eq. (C1) from the bottom surface to z, *i.e.*,

$$
\begin{aligned}
\sigma_{13} &= \partial_1 p_3 + \frac{1}{2}\partial_1 m_{12} + 2\partial_1 \tau_{113} + \frac{1}{2}\partial_3 m_{32} + \partial_3 \tau_{133} \\
&\quad - \partial_1 \int_{-h/2}^{z} (\sigma_{11} - \partial_1 p_1 - \partial_1 \tau_{111})\, dz \\
\sigma_{33} &= \partial_1 p_1 - \frac{1}{2}\partial_1 m_{32} + 2\partial_1 \tau_{133} + \partial_3 p_3 + \partial_3 \tau_{333} - -barq_{-h/2} \\
&\quad - \partial_1 \int_{-h/2}^{z} \left(\sigma_{13} + \frac{1}{2}\partial_1 m_{12} - \partial_1 \tau_{113}\right) dz
\end{aligned} \tag{D19}
$$

in which the inertia force is neglected.

Appendix E Relaxation and Creep of Simple Maxwell Materials

Relaxation

For relaxation, the deflection w0 is independent of t. The solution of Eq. (43), which satisfies the boundary conditions of Eqs. (33) and (35), is

$$
w_0 = \frac{w_0(l,t)}{1 - \frac{3}{\alpha^2 l^2} + 6\frac{\cosh(\alpha l)-1}{\alpha^3 l^3 \sinh(\alpha l)}}
3\frac{\cosh(\alpha x) + \cosh(\alpha l) - \cosh[\alpha(x-l)] - 1}{\alpha^3 l^3 \sinh(\alpha l)} + \frac{3x^2}{2l^2} - \frac{x^3}{2l^3} - \frac{3x}{\alpha^2 l^3} \tag{E1}
$$

where

$$
\alpha^2 = \frac{20}{h^2}\frac{G_0}{G_{0h}} = \frac{20}{h^2}\frac{\mu}{\mu_{0h}} \tag{E2}
$$

and $w_0(l,t) = w_0(l)$ is independent of t. Then,

$$
\frac{d^3 w_0}{dx^3} - \frac{h^2}{20}\frac{G_{0h}}{G_0}\frac{d^5 w_0}{dx^5} = -\frac{3}{l^3}[1 - \frac{3}{\alpha^2 l^2} + 6\frac{\cosh(\alpha l) - 1}{\alpha^3 l^3 \sinh(\alpha l)}]^{-1} w_0(l,t) \tag{E3}
$$

Equation (45) becomes

$$
\left(1 + \eta\frac{\partial}{\partial t}\right) Q = \frac{3G_0}{l^3}\left[1 - \frac{3}{\alpha^2 l^2} + 6\frac{\cosh(\alpha l) - 1}{\alpha^3 l^3 \sinh(\alpha l)}\right]^{-1} w_0(l) \tag{E4}
$$

The initial condition at t = 0 is

$$
\begin{aligned}
Q &= -(G_0+G_1)\left(\frac{\partial^3 w_0}{\partial x^3} - \frac{h^2}{20}\frac{G_{0h}}{G_0}\frac{\partial^5 w_0}{\partial x^5}\right) \\
&= \frac{3(1+\frac{\mu_1}{\mu})G_0}{l^3\left[1-\frac{3}{\alpha^2 l^2}+6\frac{\cosh(\alpha l)-1}{\alpha^3 l^3\sinh(\alpha l)}\right]} w_0(l)
\end{aligned}
\tag{E5}
$$

The solution of Eq. (E4) is

$$
Q(t) = \frac{3G_0}{l^3}\left[1-\frac{3}{\alpha^2 l^2}+6\frac{\cosh(\alpha l)-1}{\alpha^3 l^3\sinh(\alpha l)}\right]^{-1}\left[1+\frac{\mu_1}{\mu}\exp\left(-\frac{t}{\eta}\right)\right] w_0(l) \tag{E6}
$$

which is the relaxation relation between the beam's tip deflection, $w_0(l)$, and the applied transversal force, Q.

Creep

For creep, the transversal shear force and the moment are independent of time such that

$$Q(x,t) = \bar{Q}; \quad M(x,t) = (x-l)\bar{Q} \tag{E7}$$

where $\bar{Q}$ is the applied shear force at the free end. The deflection, w_0, is in the same form as Eq. (E1)in which $w_0(l,t)$ is now a function of time. Equation (45) becomes

$$\begin{aligned}\bar{Q} &= -G_0\left[1+\eta\left(1+\frac{\mu_1}{\mu}\right)\frac{\partial}{\partial t}\right]\left(\frac{\partial^3 w_0}{\partial x^3} - \frac{h^2}{20}\frac{G_{0h}}{G_0}\frac{\partial^5 w_0}{\partial x^5}\right)\\ &= \frac{3G_0\left[1+\eta\left(1+\frac{\mu_1}{\mu}\right)\frac{\partial}{\partial t}\right]w_0(l,t)}{l^3\left[1-\frac{3}{\alpha^2 l^2}+6\frac{\cosh(\alpha l)-1}{\alpha^3 l^3 \sinh(\alpha l)}\right]}\end{aligned} \tag{E8}$$

The initial condition for $w_0(l,t)$ is similar to Eq. (52) with Q replaced by $\bar{Q}$. The solution of Eq. (E7) is

$$w_0(l,t) = \frac{\bar{Q}l^3}{3G_0}\left[1-\frac{3}{\alpha^2 l^2}+6\frac{\cosh(\alpha l)-1}{\alpha^3 l^3 \sinh(\alpha l)}\right]\left[1-\frac{\mu_1}{\mu+\mu_1}\exp\left(-\frac{\mu}{\mu+\mu_1}\frac{t}{\eta}\right)\right] \tag{E9}$$

which is the creep relation between the deflection and the applied shear force at the tip of the beam. The moment equilibrium is

$$\begin{aligned}(1+\eta\frac{\partial}{\partial t})M = M = -(1+\eta\frac{\partial}{\partial t})D_0 D_1\frac{\partial^2 w_0}{\partial x^2} &= -[G_0+\eta(G_0+G_1)\frac{\partial}{\partial t}]\frac{\partial^2 w_0}{\partial x^2}\\ &= (x-l)\bar{Q}\end{aligned} \tag{E10}$$

Appendix F Relaxation and Creep of Simple Kelvin-Voigt Materials

For conventional simple Kelvin-Voigt materials, there are two springs in series, one of which has a parallel damper and one has no parallel damper, associated with the strains. Equation (32) becomes

$$\begin{aligned}-\frac{h^3}{6(1-\nu)}\Bigg\{&\left[\frac{\mu_1\mu(1+\eta D)}{\mu+\mu_1(1+\eta D)}+\frac{b_h^2}{h^2}\frac{\mu_{1h}\mu_{0h}(1+\eta D)}{\mu_{0h}+\mu_{1h}(1+\eta D)}\right]\frac{\partial^4 w_0}{\partial x^4}\\ &-\frac{h^2}{20}\left[\frac{\mu_1\mu(1+\eta D)}{\mu+\mu_1(1+\eta D)}+\frac{b_h^2}{h^2}\frac{\mu_{1h}\mu_{0h}(1+\eta D)}{\mu_{0h}+\mu_{1h}(1+\eta D)}\right]\frac{\partial^6 w_0}{\partial x^6}\Bigg\} = 0\end{aligned} \tag{F1}$$

where D is an differential operator of time. With materials satisfying Eq. (41), the governing equation above reduces to Eq. (55).

Relaxation

For a sudden deflection of $w_0(l)$ at $x = l$, the solution that satisfies the boundary conditions of Eqs. (33) and (34) is the same as that given in Eq. (47) with $w_0(l,t) = w_0(l)$. From Eq. (57), we obtain

$$\left(1+\frac{\mu}{\mu_1}+\eta\frac{\partial}{\partial t}\right)Q = -\left[G_0\frac{d^2w_0}{dx^2}(l)-\frac{h^2}{20}G_{0h}\frac{d^4w_0}{dx^4}(l)\right] = \frac{3G_0w_0(l)}{l^3\left[1-\frac{3}{\alpha^2l^2}+6\frac{\cosh(\alpha l)-1}{\alpha^3l^3\sinh(\alpha l)}\right]} \quad \text{(F2)}$$

Note that w_0 is independent of t. The solution for Q is

$$Q(t) = \frac{3G_0}{l^3}\left(1+\frac{\mu}{\mu_1}\right)^{-1}\left[1-\frac{3}{\alpha^2l^2}+6\frac{\cosh(\alpha l)-1}{\alpha^3l^3\sinh(\alpha l)}\right]^{-1} \left[1+\frac{\mu}{\mu_1}\exp\left(-\frac{\mu+\mu_1}{\mu_1}\frac{t}{\eta}\right)\right]w_0(l) \quad \text{(F3)}$$

for the initial condition of Eq.(58).

Creep

For a sudden applied shear force, $\bar{Q}$, at $x = l$, the creep solution that satisfies the boundary conditions, Eqs. (33) and (34), is the same as that given in Eq. (47). Equation (57)reduces to

$$\bar{Q} = -\left(1+\eta\frac{\partial}{\partial t}\right)\left[G_0\frac{d^2w_0(l,t)}{dx^2}-\frac{h^2}{20}G_{0h}\frac{d^4w_0(l,t)}{dx^4}\right] \frac{3G_0\left(1+\eta\frac{\partial}{\partial t}\right)w_0(l,t)}{l^3\left[1-\frac{3}{\alpha^2l^2}+6\frac{\cosh(\alpha l)-1}{\alpha^3l^3\sinh(\alpha l)}\right]} \quad \text{(F4)}$$

which gives the creep relation between the tip deflection and the applied shear force,

$$w_0(l,t) = \frac{\bar{Q}l^3}{3G_0}\left[1-\frac{3}{\alpha^2l^2}+6\frac{\cosh(\alpha l)-1}{\alpha^3l^3\sinh(\alpha l)}\right]\left[1+\frac{\mu}{\mu_1}-\frac{\mu}{\mu_1}\exp\left(-\frac{t}{\eta}\right)\right] \quad \text{(F5)}$$

Acknowledgement: This work was supported by the Research Grants Council of the Hong Kong Special Administrative Region, the People's Republic of China under projects HKUST6190/03E; 615007; 615505).

References

Arinstein, A.; Burman, M.; Gendelman; O. Zussman; E. (2007): Effect of supramolecular structure on polymer nanofibre elasticity. *Nature Nanotechnology* 2(2), 59-62.

Cuenot, S.; Demoustier-Champagne, S.; Nysten. B. (2000): Elastic modulus of polypyrrole nanotubes. *Physical Review Letters* 85, 1690-1693.

Cuenot, S.; Frétigny, C.; Demoustier-Champagne, S. (2004): Surface tension effect on the mechanical properties of nanomaterials measured by atomic force microscopy. *Physical Review B* 69, 165410-165414.

Doi, M. (1996): Introduction to polymer physics, Claendon Press, Oxford.

Fleck, N.A.; Muller, G. M.; Ashby, M. F.; Hutchinson, J. W. (1994): Strain gradient plasticity: theory and experiment. *Acta Metallurgica et Materialia.* 42(2), 475-487.

Fung, Y.C..; Tong, P. (2001): Chapter 15, *Classical and Computational Solid Mechanics*, World Scientific, Hong Kong.

Gu, S. Y.; Wu, Q. L.; Ren, J.; Vancso, G. J. (2005): Mechanical properties of a single electrospun fiber and its structures. *Macromolecular Rapid Communications* 26(9), 716-720.

Ji, Y.; Li, B.; Ge, S.; Sokolov, J. C.; Rafailovich, M. H. (2006): Structure and Nanomechanical Characterization of Electrospun PS/Clay Nanocomposite Fibers. *Langmuir* 22(3), 1321-1328.

Lam, D. C. C.; Chong, A. C. M. (1999): Indentation model and strain gradient plasticity law for glassy polymers. *Journal of Materials Research* 14(9), 3784.

Lam, D. C. C.; Yang, Y.; Chong, A. C. M.; Wang, J.; Tong, P. (2003): Experiments and theory in strain gradient elasticity. *Journal of the Mechanics and Physics of Solids* 51(8), 1477-1508.

McFarland, A. W.; Colton, J. S. (2005): Role of material microstructure in plate stiffness with relevance to microcantilever sensors. *Journal of Micromechanics and Microengineering* 15(5), 1060-1067.

Treloar, L. R. G. (2005): The physics of rubber elasticity, 3rd ed. Clarendon Press, Oxford.

Wei., W.; Lam, D.C.C. (2010): *CMES: Computer Modeling in Engineering & Science* 1708 (1) 1-14.

Wang, J.; Lam, D.C.C. (2010): *CMC: Computers, Materials and Continua* 471 (1) 1-18.